

Mobile-Former: Bridging MobileNet and Transformer

Yinpeng Chen¹ Xiyang Dai¹ Dongdong Chen¹ Mengchen Liu¹ Xiaoyi Dong²
 Lu Yuan¹ Zicheng Liu¹

¹ Microsoft

² University of Science and Technology of China

{yiche, xidai, dochen, mengcliu, luyuan, zliu}@microsoft.com,

dlight@mail.ustc.edu.cn

Abstract

We present *Mobile-Former*, a parallel design of *MobileNet* and *Transformer* with a two-way bridge in between. This structure leverages the advantage of *MobileNet* at local processing and *transformer* at global interaction. And the bridge enables bidirectional fusion of local and global features. Different with recent works on vision transformer, the transformer in *Mobile-Former* contains very few tokens (e.g. less than 6 tokens) that are randomly initialized, resulting in low computational cost. Combining with the proposed light-weight cross attention to model the bridge, *Mobile-Former* is not only computationally efficient, but also has more representation power, outperforming *MobileNetV3* at low FLOP regime from 25M to 500M FLOPs on ImageNet classification. For instance, it achieves 77.9% top-1 accuracy at 294M FLOPs, gaining 1.3% over *MobileNetV3* but saving 17% of computations. When transferring to object detection, *Mobile-Former* outperforms *MobileNetV3* by 8.6 AP.

1. Introduction

Recently, Vision Transformer (ViT) [8, 29] demonstrates the advantage of global processing and achieves significant performance boost over CNNs. However, when constraining the computational budget within 1G FLOPs, the gain of ViT diminishes. If we further challenge the computational cost, *MobileNet* [14, 15, 24] and its extensions [10, 17] still dominate their backyard (e.g. less than 300M FLOPs for ImageNet classification) due to their efficiency in local processing filters via decomposition of depthwise and pointwise convolution. This in turn naturally raises a question:

How to design efficient networks to effectively encode both local processing and global interaction?

A straightforward idea is to combine convolution and vision transformer. Recent works [9, 35, 36] show the benefit of

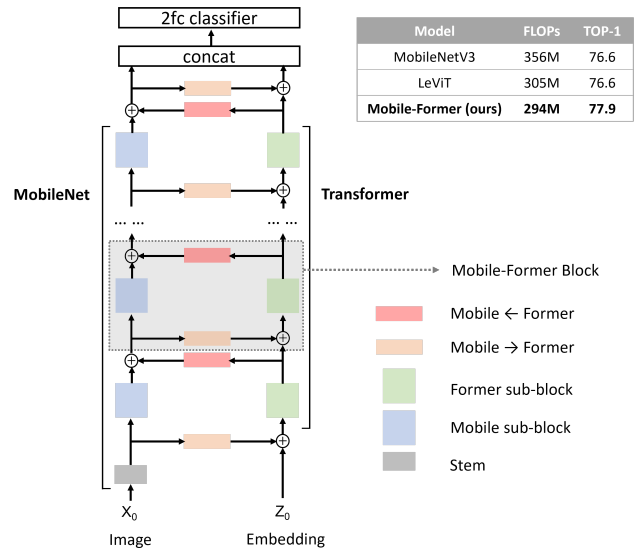


Figure 1. **Overview of Mobile-Former**, which parallelizes *MobileNet* [24] (on the left side) and *Transformer* [33] (on the right side). Different with vision transformer [8] that uses image patches to form tokens, the transformer in *Mobile-Former* takes very few learnable tokens as input that are randomly initialized. *Mobile* (refers to *MobileNet*) and *Former* (refers to transformer) are communicated by a bidirectional bridge, which is modeled by the proposed light-weight cross attention. Best viewed in color.

combining convolution and vision transformer in *series*, either using convolution at the beginning or intertwining convolution into each transformer block.

In this paper, we shift the design paradigm from *series* to *parallel*, and propose a new network that parallelizes *MobileNet* and transformer with a two-way bridge in between (see Figure 1). We name it *Mobile-Former*, where *Mobile* refers to *MobileNet* and *Former* stands for transformer. *Mobile* takes the image as input and stacks mobile (or inverted bottleneck) blocks [24]. It leverages the efficient depthwise and pointwise convolution to extract local features at pixel level. *Former* takes a few learnable tokens as input

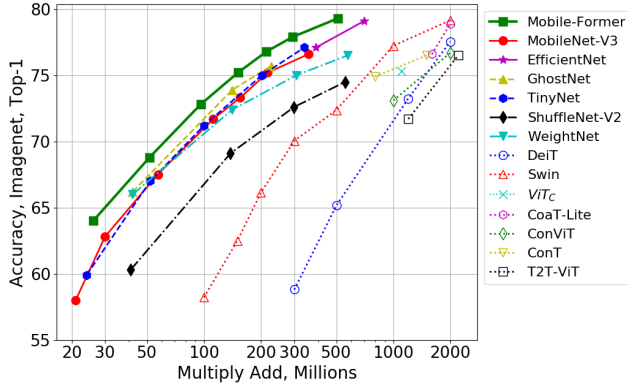


Figure 2. **Comparison among Mobile-Former, efficient CNNs and Vision Transformers**, in terms of accuracy-flop tradeoff. The comparison is performed on ImageNet classification. Mobile-Former consistently outperforms both efficient CNNs and vision transformers in low FLOP regime (from 25M to 500M MAAdd). Note that we implement Swin [20] and DeiT [29] at low computational budget from 100M to 2G FLOPs. Best viewed in color.

and stacks multi-head attention and feed-forward networks (FFN). These tokens are used to encode global features of the image.

Mobile and *Former* communicate over a two-way bridge to fuse local and global features. This is crucial since it feeds local features to *Former*'s tokens as well as introduces global views to every pixel of featuremap in *Mobile*. We propose a light-weight cross attention to model this bidirectional bridge by (a) performing the cross attention at the bottleneck of *Mobile* where the number of channel is low, and (b) removing projections on query, key and value (W^Q , W^K , W^V) from *Mobile* side.

This parallel structure with a bidirectional bridge leverages the advantage of both MobileNet and transformer. The decoupling of local and global features in parallel leverage MobileNet's efficiency in extracting local features as well as transformer's power in modeling global interaction. More important, this is achieved in an efficient way via a thin transformer (with very few tokens) and a light-weight bridge to exchange local and global features between *Mobile* and *Former*. The bridge and *Former* consumes less than 20% of the total computational cost, but significantly improve the representation capability. This showcases an efficient and effective implementation of part-whole hierarchy proposed in [13].

Mobile-Former achieves solid performance on both image classification and object detection. For example, it achieves 77.9% top-1 ImageNet accuracy at 294M FLOPs, outperforming MobileNetV3 [14] and LeViT [9] by a clear margin (see Figure 1). More important, Mobile-Former consistently outperforming both efficient CNNs and vision transformers from 25M to 500M FLOPs (shown in Fig-

ure 2), showcasing the usage of transformer at the low FLOP regime where efficient CNNs dominate. Furthermore, when transferring from Image classification to object detection, Mobile-Former significantly outperforms MobileNetV3, e.g. gaining 8.6 AP (35.8 vs. 27.2) with even less computational cost.

Finally we note that *exploring the optimal network parameters (e.g. width, height) in Mobile-Former is not a goal of this work*, rather we demonstrate that the parallel design of Mobile-Former provides an efficient and effective network architecture.

2. Related Work

Light-weight Convolutional Neural Networks (CNNs):

MobileNets [14, 15, 24] proposes an efficient way to model local filter processing by using depthwise and pointwise convolution in an inverted bottleneck structure. [23, 42] proposes ShuffleNet that uses group convolution and channel shuffle to simplify pointwise convolution. Furthermore, MicroNet [17] presents micro-factorized convolution that optimizes the combination of inverted bottleneck and group convolution and achieves solid performance at extremely low FLOPs. Dynamic operators [2, 3, 16, 39] have been studied to boost performance for MobileNet with negligible computational cost. Other efficient operators include butterfly transform [31], cheap linear transformations in GhostNet [10], and using cheap additions to trade massive multiplications in AdderNet [1]. In addition, different architectures and compound scaling method have been studied. MixConv [27] explores mixing up multiple kernel sizes, and Sandglass [44] flips the structure of inverted residual block. EfficientNet [26, 28] and TinyNet [11] study the compound scaling of depth, width and resolution.

Vision Transformers (ViT):

Recently, ViT [8] and its follow-ups [7, 20, 29, 32, 40] achieve impressive performance on multiple vision tasks. The original ViT requires training on large dataset such as JFT-300M to perform well. Later, DeiT [29] demonstrates that good performance can be achieved on the smaller ImageNet-1K dataset by introducing several important training strategies. To enable ViT for high resolution images, several hierarchical transformers are proposed. For example, Swin [20] presents shifted window approach for computing self-attention within a local window and CSWin [7] further improves it by introducing cross-shaped window self-attention. T2T-ViT [40] progressively converts the image to tokens by recursively aggregating neighboring tokens, such that the local structure can be well modeled. HaloNet [32] develops two attention extensions (blocked local attention and attention downsampling) that result in improvement of speed, memory usage and accuracy.

Combination of CNNs and ViT: Recent works [5, 9, 25,

[35, 36] show that combining convolution and transformer achieves improvement in prediction accuracy as well as training stability. BoTNet [25] shows significant improvement in instance segmentation and object detection by just replacing the spatial convolutions with global self-attention in the final three bottleneck blocks of a ResNet [12]. ConViT [5] improves ViT with soft convolutional inductive biases by introducing a gated positional self-attention (GPSA). CvT [35] introduces depthwise/pointwise convolution before each multi-head attention. LeViT [9] and ViT_C [36] use convolutional stem (stacking 3×3 convolutions) to replace the patchify stem [36]. LeViT and ViT_C show clear improvement at the low FLOP regime. In this paper, we propose a different design that parallelizes MobileNet and transformer with bidirectional cross attention in between. Our approach is both efficient and effective, outperforming both efficient CNNs and ViT variants at low FLOP regime.

3. Our Method: Mobile-Former

In this section, we describe the design process of Mobile-Former and its building blocks. The architecture is summarized in Figure 1 and Figure 3.

3.1. Overview

Mobile-Former parallelizes MobileNet and transformer, and connects them by bidirectional cross attention (see Figure 1). In Mobile-Former, *Mobile* (refers to MobileNet) takes an image as input ($\mathbf{X}_0 \in \mathbb{R}^{H \times W \times 3}$) and applies inverted bottleneck blocks [24] to extract local features. *Former* (refers to transformer) takes learnable parameters (or tokens) as input, denoted as $\mathbf{Z}_0 \in \mathbb{R}^{M \times d}$ where d and M are the dimension and number of tokens, respectively. These tokens are randomly initialized and each represents a global prior of the image. This is different with Vision Transformer (ViT) [8], where tokens project the local image patch linearly. This difference is important as it significantly reduces the number of tokens ($M \leq 6$ in this paper), resulting in an efficient *Former*.

Mobile and *Former* are connected by a two-way bridge where local and global features are fused bidirectionally. Here, we denote two directions of the bridge as *Mobile*→*Former* and *Mobile*←*Former*, respectively. We propose a light-weight cross attention to model this bidirectional bridge, which will be discussed next.

3.2. Low Cost Two-Way Bridge

We leverage the advantage of cross attention to fuse the local features (from *Mobile*) and global tokens (from *Former*). Here, two changes are introduced to the standard cross attention for the sake of low computational cost: (a) computing the cross attention at the bottleneck of *Mobile* where the number of channels is low, and (b) removing the

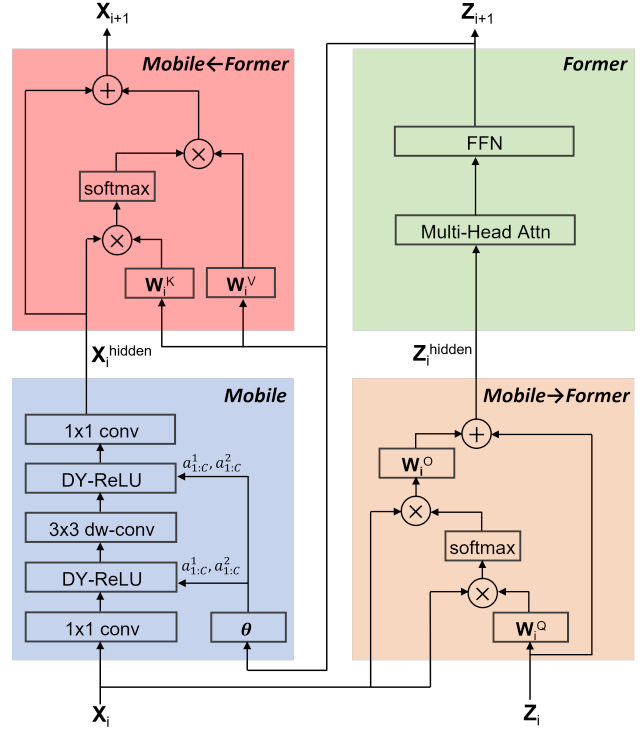


Figure 3. **Mobile-Former Block** that includes four modules: *Mobile* sub-block modifies inverted bottleneck block in [24] by replacing ReLU with dynamic ReLU [3]. *Mobile*→*Former* uses light-weight cross attention to fuse local features into global features. *Former* sub-block is a standard transformer block including multi-head attention and FFN. Note that the output of *Former* is used to generate parameters for dynamic ReLU in *Mobile* sub-block. *Mobile*←*Former* bridges from global to local features.

projections ($\mathbf{W}_i^Q, \mathbf{W}_i^K, \mathbf{W}_i^V$) from *Mobile* side where the number of positions is large, but keeping them at *Former* side.

Let us denote the local feature map as \mathbf{x} , and the global tokens as \mathbf{z} . They are split as $\mathbf{x} = [\mathbf{x}_h]$ and $\mathbf{z} = [\mathbf{z}_h]$ ($1 \leq h \leq H$) for multi-head attention with H heads. The light-weight cross attention from local to global is defined as follows:

$$\mathbf{z}^{out} = \mathbf{z} + \left[\text{Attention}(\mathbf{z}_h \mathbf{W}_h^Q, \mathbf{x}_h, \mathbf{x}_h) \right]_{h=1:H} \mathbf{W}^O, \quad (1)$$

where \mathbf{W}_h^Q is the query projection matrix in the h^{th} head, \mathbf{W}^O is used to combine multiple heads together, $\text{Attention}(Q, K, V)$ is the standard attention function (in [33]) over query Q , key K , and value V as follows:

$$\text{Attention}(Q, K, V) = \text{softmax}\left(\frac{QK^T}{\sqrt{d_k}}\right)V. \quad (2)$$

Note that the global feature \mathbf{z} is the query and the local feature \mathbf{x} is the key and value. \mathbf{W}_h^Q and \mathbf{W}^O are applied

on global tokens z . The diagram of this cross attention is shown in Figure 3 (*Mobile*→*Former*).

In a similar manner, the cross attention from global to local is computed as:

$$\mathbf{x}^{out} = \mathbf{x} + \left[\text{Attention}(\mathbf{x}_h, \mathbf{z}_h \mathbf{W}_h^K, \mathbf{z}_h \mathbf{W}_h^V) \right]_{h=1:H}, \quad (3)$$

where \mathbf{W}_h^K and \mathbf{W}_h^V are the projection matrices for key and value. Here, the local feature \mathbf{x} is the query and the global feature \mathbf{z} is the key and value. The diagram of this cross attention is shown in Figure 3 (*Mobile*←*Former*).

3.3. Mobile-Former Block

Mobile-Former can be decoupled as a stack of *Mobile-Former blocks* (see Figure 1). Each block includes a *Mobile* sub-block, a *Former* sub-block, and a bidirectional bridge (*Mobile*←*Former* and *Mobile*→*Former*). The details of Mobile-Former block are shown in Figure 3.

Input and Output: Mobile-Former block has two inputs: (a) local feature map $\mathbf{X}_i \in \mathbb{R}^{L \times C}$, which has C channels and L spatial positions ($L = hw$ where h and w are the height and width of the feature map), and (b) global tokens $\mathbf{Z}_i \in \mathbb{R}^{M \times d}$, where M and d are the number and dimension of tokens, respectively. Mobile-Former block outputs the updated local feature map \mathbf{X}_{i+1} and global tokens \mathbf{Z}_{i+1} , which are used as input for the next ($i+1^{th}$) block. Note the number and dimension of global tokens are identical across all blocks.

Mobile sub-block: *Mobile* sub-block takes feature map \mathbf{X}_i as input. It is slightly different to the inverted bottleneck block in [24] by replacing ReLU with dynamic ReLU [3] as the activation function after the first pointwise convolution and the 3×3 depthwise convolution. Different with the original dynamic ReLU, in which the parameters are generated by applying two MLP layers on the average pooled feature, we save the average pooling by applying the two MLP layers (θ in Figure 3) on the first global token output from *Former*. Note that the kernel size of depthwise convolution is 3×3 for all blocks. The output of *Mobile* sub-block, denoted as \mathbf{X}_i^{hidden} , is taken as the input for *Mobile*←*Former* (see Figure 3). Its computational complexity is $O(2LEC^2 + 9LEC)$, where L is the number of spatial positions, E is the channel expansion ratio, and C is the number of channels before the expansion.

Former sub-block: *Former* sub-block is a standard transform block with a multi-head attention (MHA) and a feed-forward network (FFN). Here, we follow [33] to use post layer normalization. To save computations, we use expansion ratio 2 instead of 4 in FFN. Note that *Former* sub-block is processed between the two-way cross attention, i.e. after *Mobile*→*Former* and before *Mobile*←*Former* (see Figure 3). Its complexity is $O(M^2d + Md^2)$. The first item

relates to computing dot product between query and key, and aggregating values based on attention values, while the second item covers linear projections and FFN. Since *Former* only has a few tokens ($M \leq 6$), the first item M^2d is ignorable.

Mobile→**Former:** The proposed light-weight cross attention (Equation 1) is used to fuse local features \mathbf{X}_i to global tokens \mathbf{Z}_i . Compared to the standard attention, the projection matrices for key \mathbf{W}^K and value \mathbf{W}^V (on the local features) are removed to save computations (shown in Figure 3). Its computational complexity is $O(LMC + MdC)$, where the first item relates to computing cross attention between local and global features and aggregating local features for each global token, and the second item is the complexity to project global features to the same dimension of local features C and back to dimension d after aggregation.

Mobile←**Former:** Here, the cross attention (Equation 3) is on the opposite direction to *Mobile*→*Former*. It fuses global tokens \mathbf{Z}_i to local features \mathbf{X}_i . The local features are the query and global tokens are key and value. Therefore, we keep the projection matrices for key \mathbf{W}^K and value \mathbf{W}^V , but remove the projection matrix for query \mathbf{W}^Q to save computations, as shown in Figure 3. The computational complexity is $O(LMC + MdC)$.

Computational Complexity: The four pillars of Mobile-Former block have different computational costs. *Mobile* sub-block consumes the most computations ($O(2LEC^2 + 9LEC)$), as it grows linearly with the number of spatial positions L and grows quadratically with the number of channels in local features C . *Former* sub-block and the two-way bridge are computational efficient, consuming less than 20% of total computation for all Mobile-Former models.

3.4. Network Specification

Architecture: Table 1 shows a Mobile-Former architecture at 294M FLOPs, which stacks 11 Mobile-Former blocks at different input resolutions. All Mobile-Former blocks have 6 global tokens with dimension 192. It starts with a 3×3 convolution as stem which is followed by a lite bottleneck block at stage 1. The lite bottleneck block is proposed in [17], which uses a 3×3 depthwise convolution to expand the number of channels and uses a pointwise convolution to squeeze the number of channels. The classification head applies average pooling on the local features, concatenates with the first global token, and then passes through two fully connected layers with h-swish [14] in between.

Downsample Mobile-Former Block: Note that stage 2–5 has a downsample variant of Mobile-Former block (denoted as *Mobile-Former*[↓]) to handle the spatial downsampling. In *Mobile-Former*[↓], only the convolution layers in *Mobile* sub-block are changed from three lay-

Stage	Input	Operator	exp size	#out	Stride
tokens	6×192	–	–	–	–
stem	$224^2 \times 3$	conv2d, 3×3	–	16	2
1	$112^2 \times 16$	bneck-lite	32	16	1
2	$112^2 \times 16$	Mobile-Former \downarrow	96	24	2
	$56^2 \times 24$	Mobile-Former	96	24	1
3	$56^2 \times 24$	Mobile-Former \downarrow	144	48	2
	$28^2 \times 48$	Mobile-Former	192	48	1
4	$28^2 \times 48$	Mobile-Former \downarrow	288	96	2
	$14^2 \times 96$	Mobile-Former	384	96	1
	$14^2 \times 96$	Mobile-Former	576	128	1
	$14^2 \times 128$	Mobile-Former	768	128	1
5	$14^2 \times 128$	Mobile-Former \downarrow	768	192	2
	$7^2 \times 192$	Mobile-Former	1152	192	1
	$7^2 \times 192$	Mobile-Former	1152	192	1
	$7^2 \times 192$	conv2d, 1×1	–	1152	1
head	$7^2 \times 1152$	pool, 7×7	–	–	1
	$1^2 \times 1152$	concat w/ cls token	–	1344	1
	$1^2 \times 1344$	FC	–	1920	1
	$1^2 \times 1920$	FC	–	1000	1

Table 1. **Specification for Mobile-Former-294M.** “bneck-lite” denotes light bottleneck block. “Mobile-Former \downarrow ” denotes the Mobile-Former block for downsampling.

ers (pointwise \rightarrow depthwise \rightarrow pointwise) to four layers (depthwise \rightarrow pointwise \rightarrow depthwise \rightarrow pointwise), where the first depthwise convolution layer has stride 2. The number of channels expands in each depthwise convolution, and squeezes in the following pointwise convolution. This saves computations as the two costly pointwise convolutions are performed at the lower resolution after downsampling.

Mobile-Former Variants: Mobile-Former has 7 models of different computational costs from 26M to 508M FLOPs. They share the similar architecture, but have different widths and heights. We follow [36] to refer our models by their flops, e.g. Mobile-Former-294M, Mobile-Former-96M. The details of network architecture for these Mobile-Former models are listed in the appendix (see Table 10).

4. Experimental Results

We conduct experiments on ImageNet classification [6], and COCO object detection [19] to evaluate the proposed Mobile-Former.

4.1. ImageNet Classification

We now evaluate our Mobile-Former models on ImageNet [6] classification. ImageNet has 1000 classes, including 1,281,167 images for training and 50,000 images for validation.

Training Setup: The image resolution is 224×224 . All models are trained from scratch using AdamW [21] optimizer for 450 epochs with cosine learning rate decay. A

Model	Input	#Param	MAdds	Top-1
MobileNetV3 Small $1.0 \times$ [14]	160^2	2.5M	30M	62.8
Mobile-Former-26M	224^2	3.2M	26M	64.0
MobileNetV3 Small $1.0 \times$ [14]	224^2	2.5M	57M	67.5
Mobile-Former-52M	224^2	3.5M	52M	68.7
MobileNetV3 $1.0 \times$ [14]	160^2	5.4M	112M	71.7
Mobile-Former-96M	224^2	4.6M	96M	72.8
ShuffleNetV2 $1.0 \times$ [23]	224^2	2.2M	138M	69.1
ShuffleNetV2 $1.0 \times$ +WeightNet $4 \times$ [22]	224^2	5.1M	141M	72.4
MobileNetV3 $0.75 \times$ [14]	224^2	4.0M	155M	73.3
Mobile-Former-151M	224^2	7.6M	151M	75.2
MobileNetV3 $1.0 \times$ [14]	224^2	5.4M	217M	75.2
Mobile-Former-214M	224^2	9.4M	214M	76.7
ShuffleNetV2 $1.5 \times$ [23]	224^2	3.5M	299M	72.6
ShuffleNetV2 $1.5 \times$ +WeightNet $4 \times$ [22]	224^2	9.6M	307M	75.0
MobileNetV3 $1.25 \times$ [14]	224^2	7.5M	356M	76.6
EfficientNet-B0 [26]	224^2	5.3M	390M	77.1
Mobile-Former-294M	224^2	11.4M	294M	77.9
ShuffleNetV2 $2 \times$ [23]	224^2	5.5M	557M	74.5
ShuffleNetV2 $2 \times$ +WeightNet $4 \times$ [22]	224^2	18.1M	573M	76.5
Mobile-Former-508M	224^2	14.0M	508M	79.3

Table 2. **Comparing Mobile-Former with efficient CNNs** evaluated on ImageNet [6] classification.

batch size of 1024 is used. Data augmentation includes Mixup [41], auto-augmentation [4], and random erasing [43]. Different combinations of initial learning rate, weight decay and dropout are used for models with different complexities, which are listed in the appendix (see Table 11).

Main Results: Table 2 shows the comparison between Mobile-Former and classic efficient CNNs: (a) MobileNetV3 [14], (b) EfficientNet [26], and (c) ShuffleNetV2 [23] and its extension WeightNet [22]. The comparison covers the FLOP range from 26M to 508M, organized in seven groups based on similar FLOPs. Mobile-Former consistently outperforms efficient CNNs with even less computational cost except the group around 150M FLOPs, where Mobile-Former costs slightly more FLOPs than ShuffleNet/WeightNet (151M vs. 138M/141M), but achieves significantly higher top-1 accuracy (75.2% vs. 69.1%/72.4%). This demonstrates that our parallel design improves the representation capability efficiently.

In Table 3, we compare Mobile-Former with multiple variants (DeiT [29], T2T-ViT [40], PVT [34], ConViT [5], CoaT [37], ViT_C [36], Swin [20]) of vision transformer. All variants use image resolution 224×224 and are trained *without* distillation from a teacher network. Mobile-Former achieves higher accuracy but uses 3~4 times less computational cost. This is because that Mobile-Former uses significantly fewer tokens to model global interaction and leverages MobileNet to extract local features efficiently. Note that our Mobile-Former (trained in 450 epochs without distillation) even outperforms LeViT [9] which leverages the distillation of a teacher network and much longer training (1000 epochs). Our method achieves higher top-1 accuracy

Model	Input	#Param	MAdds	Top-1
T2T-ViT-7 [40]	224 ²	4.3M	1.2G	71.7
DeiT-Tiny [29]	224 ²	5.7M	1.2G	72.2
ConViT-Tiny [5]	224 ²	6.0M	1.0G	73.1
ConT-Ti [38]	224 ²	5.8M	0.8G	74.9
ViT _C [36]	224 ²	4.6M	1.1G	75.3
ConT-S [38]	224 ²	10.1M	1.5G	76.5
Swin-1G [20] ‡	224 ²	7.3M	1.0G	77.3
Mobile-Former-294M	224 ²	11.4M	294M	77.9
PVT-Tiny [34]	224 ²	13.2M	1.9G	75.1
T2T-ViT-12 [40]	224 ²	6.9M	2.2G	76.5
CoaT-Lite Tiny [37]	224 ²	5.7M	1.6G	76.6
ConViT-Tiny+ [5]	224 ²	10.0M	2G	76.7
DeiT-2G [29] ‡	224 ²	9.5M	2.0G	77.6
CoaT-Lite Mini [37]	224 ²	11.0M	2.0G	78.9
BoT-S1-50 [25]	224 ²	20.8M	4.3G	79.1
Swin-2G [20] ‡	224 ²	12.8M	2.0G	79.2
Mobile-Former-508M	224 ²	14.0M	508M	79.3

Table 3. **Comparing Mobile-Former with Vision Transformer variants** evaluated on ImageNet [6] classification. Here, we choose ViT variants that use image resolution 224×224 and are trained *without* distillation from a teacher network. We split ViT models based on FLOPs (using 1.5G as threshold) and rank them based on top-1 accuracy. ‡ indicates our implementation.

(77.9% vs. 76.6%) but uses less computation (294M vs. 305M FLOPs) than LeViT.

Figure 2 compares Mobile-Former with more efficient CNNs (e.g. GhostNet [10]) and vision transformer variants with lower FLOPs (e.g. Swin [20] and DeiT [29] from 100M to 2G FLOPs). Note that we implement Swin and DeiT for the low computational budget from 100M to 2G FLOPs, by carefully reducing the network width and height. Mobile-Former clearly outperforms both CNNs and ViT variants, demonstrating the advantage of the parallel design to integrate MobileNet and transformer. Although vision transformers are inferior to efficient CNNs by a large margin, our work showcases that the transformer can also contribute to the low FLOP regime with proper architecture design.

4.2. Object Detection

Object detection experiments are conducted on COCO 2017 [19], which contains 118K training and 5K validation images. We use RetinaNet [18] (one-stage) as the detection framework and follow the standard settings to use our Mobile-Former as backbone to generate feature map at multiple scales. All models are trained for 12 epochs (1×) from ImageNet pretrained weights.

In Table 4, we compare Mobile-Former with both CNNs (ResNet [12], MobileNetV3 [14], ShuffleNetV2 [23]) and vision transformers (PVT [34] and ConT [38]). Mobile-Former significantly outperforms MobileNetV3 and ShuffleNet by 8.3+ AP under similar computational cost. Compared to ResNet and vision transform variants, our Mobile-

Former achieves higher AP with significantly less FLOPs in the backbone. Specifically, our Mobile-Former-508M only takes 9.4G FLOPs in backbone but achieves 38.0 AP, outperforming ResNet-50, PVT-Tiny, and ConT-M which consume 7 times more computation (65G to 84G FLOPs) in the backbone. This demonstrates that Mobile-Former is also effective and efficient in the object detection task.

5. Ablations and Discussion

In this section, we show Mobile-Former is effective and efficient via several ablations performed on ImageNet classification. Here, Mobile-Former-294M is used and all models are trained for 300 epochs. Moreover, we visualize the two-way cross attention to understand the communication between *Mobile* and *Former*. Finally, the limitations of Mobile-Former are discussed.

5.1. Mobile-Former is Effective

Mobile-Former is more effective than MobileNet as it encodes global interaction via *Former*, resulting in more accurate prediction. As shown in Table 5, adding *Former* and bridge (*Mobile*→*Former* and *Mobile*←*Former*) only costs 10.6% of the computational cost, but gains 2.6% top-1 accuracy over the baseline that uses *Mobile* alone. In addition, using the first global token to generate parameters for dynamic ReLU [3] in *Mobile* sub-block (see Figure 3) achieves additional 1.0% top-1 accuracy. This validates our parallel design in Mobile-Former.

We also perform another ablation on the kernel size of the depthwise convolution in *Mobile*, to validate the contribution of *Former* and bridge on global interaction. Table 6 shows that the gain of increasing kernel size (from 3×3 to 5×5) is negligible. We believe this is because *Former* and the bridge enlarge the reception field for *Mobile* via fusing global features. Therefore, using larger kernel size is not necessary in Mobile-Former.

5.2. Mobile-Former is Efficient

Mobile-Former is not only effective in encoding both local processing and global interaction, but achieves this *efficiently*. The key finding is that *Former only requires a small number of global tokens*. Here, we first show Mobile-Former is efficient in terms of both the number of tokens and dimension. Then, we show the efficient parallel design of Mobile-Former is stable when removing FFN in *Former* and replacing multi-head attention (MHA) with MLP.

Number of tokens in *Former*: Table 7 shows the ImageNet classification results for using different number of global tokens in *Former*. The token dimension is 192. Interestingly, even a single global token achieves a good performance (77.1% top-1 accuracy). Additional improvement (0.5% and 0.7% top-1 accuracy) is achieved when using

Model	AP	AP ₅₀	AP ₇₅	AP _S	AP _M	AP _L	MAdds (G)		#Params (M)	
							backbone	all	backbone	all
ShuffleNetV2 [23]	25.9	41.9	26.9	12.4	28.0	36.4	2.6	161	0.8	10.4
Mobile-Former-151M	34.2	53.4	36.0	19.9	36.8	45.3	2.4	161	4.9	14.4
MobileNetV3 [14]	27.2	43.9	28.3	13.5	30.2	37.2	4.7	162	2.8	12.3
Mobile-Former-214M	35.8	55.4	38.0	21.8	38.5	46.8	3.6	162	5.7	15.2
ResNet18 [12]	31.8	49.6	33.6	16.3	34.3	43.2	29	181	11.2	21.3
Mobile-Former-294M	36.6	56.6	38.6	21.9	39.5	47.9	5.2	164	6.5	16.1
ResNet50 [12]	36.5	55.4	39.1	20.4	40.3	48.1	84	239	23.3	37.7
PVT-Tiny [34]	36.7	56.9	38.9	22.6	38.8	50.0	70	221	12.3	23.0
ConT-M [38]	37.9	58.1	40.2	23.0	40.6	50.4	65	217	16.8	27.0
Mobile-Former-508M	38.0	58.3	40.3	22.9	41.2	49.7	9.4	168	8.4	17.9

Table 4. **COCO object detection results.** All models are trained on train2017 and tested on val2017. All models are trained for 12 epochs (1×) from ImageNet pretrained weights.

Model	#Param	MAdds	Top-1	Top-5
<i>Mobile</i> (using ReLU)	6.1M	259M	74.2	91.8
+ <i>Former</i> and Bridge	10.1M	290M	76.8 _(+2.6)	93.2 _(+1.4)
+ DY-ReLU in <i>Mobile</i>	11.4M	294M	77.8 _(+1.0)	93.7 _(+0.5)

Table 5. **Ablation of Former, Bridge and DY-ReLU** evaluated on ImageNet classification. Mobile-Former-294M is used.

Kernel Size in Mobile	#Param	MAdds	Top-1	Top-5
3×3	11.4M	294M	77.8	93.7
5×5	11.5M	332M	77.9	93.9

Table 6. **Ablation of kernel size of depthwise convolution in Mobile** evaluated on ImageNet classification. Mobile-Former-294M is used.

#tokens	#Param	MAdds	Top-1	Top-5
1	11.4M	269M	77.1	93.2
3	11.4M	279M	77.6	93.6
6	11.4M	294M	77.8	93.7
9	11.4M	309M	77.7	93.8

Table 7. **Ablation of number of tokens** on ImageNet classification. Mobile-Former-294M is used.

3 and 6 tokens. But the improvement stops when more than 6 tokens are used. This ablation shows the compactness of global tokens which is important to the efficiency of Mobile-Former.

Token Dimension: Table 8 shows the results for different token lengths (or dimension). Here, six global tokens are used in *Former*. The performance keeps improving from 76.8% to 77.8% when token dimension increases from 64 to 192, but converges when higher dimension is used. This further supports the efficiency of *Former*. When using six tokens with dimension 192, the total computational cost of *Former* and the bridge only consumes 12% of the overall budget (35M/294M).

Token Dimension	#Param	MAdds	Top-1	Top-5
64	7.3M	277M	76.8	93.1
128	9.1M	284M	77.3	93.5
192	11.4M	294M	77.8	93.7
256	14.3M	308M	77.8	93.7
320	17.9M	325M	77.6	93.6

Table 8. **Ablation of token dimension** on ImageNet classification. Mobile-Former-294M is used.

Attention	FFN	#Param	MAdds	Top-1	Top-5
MHA	✓	11.4M	294M	77.8	93.7
MHA	✗	9.8M	284M	77.5	93.6
MLP	✓	10.5M	284M	77.3	93.5

Table 9. **Ablation of multi-head attention (MHA) and FFN** evaluated on ImageNet classification. Mobile-Former-294M is used.

FFN in Former: As shown in Table 9, removing FFN introduces a small drop in top-1 accuracy (-0.3%). Compared to the important role of FFN in the original vision transformer, FFN has limited contribution in Mobile-Former. We believe this is because FFN is not the only module for channel fusion in Mobile-Former. The 1×1 convolution in *Mobile* helps the channel fusion of local features, while the projection matrix W^O in *Mobile*→*Former* (see Equation 1) contributes to the fusion between local and global features.

Multi-head Attention (MHA) vs. MLP: Table 9 shows the result of replacing multi-head attention (MHA) with MLP in both *Former* and bridge (*Mobile*→*Former* and *Mobile*←*Former*). The top-1 accuracy drops from 77.8% to 77.3%. The implementation of MLP is more efficient by a single matrix multiplication, but it is static (i.e. not adaptive to different input images).

5.3. Mobile-Former is Explainable

To understand the collaboration between *Mobile* and *Former*, we visualize the cross attention on the two-way

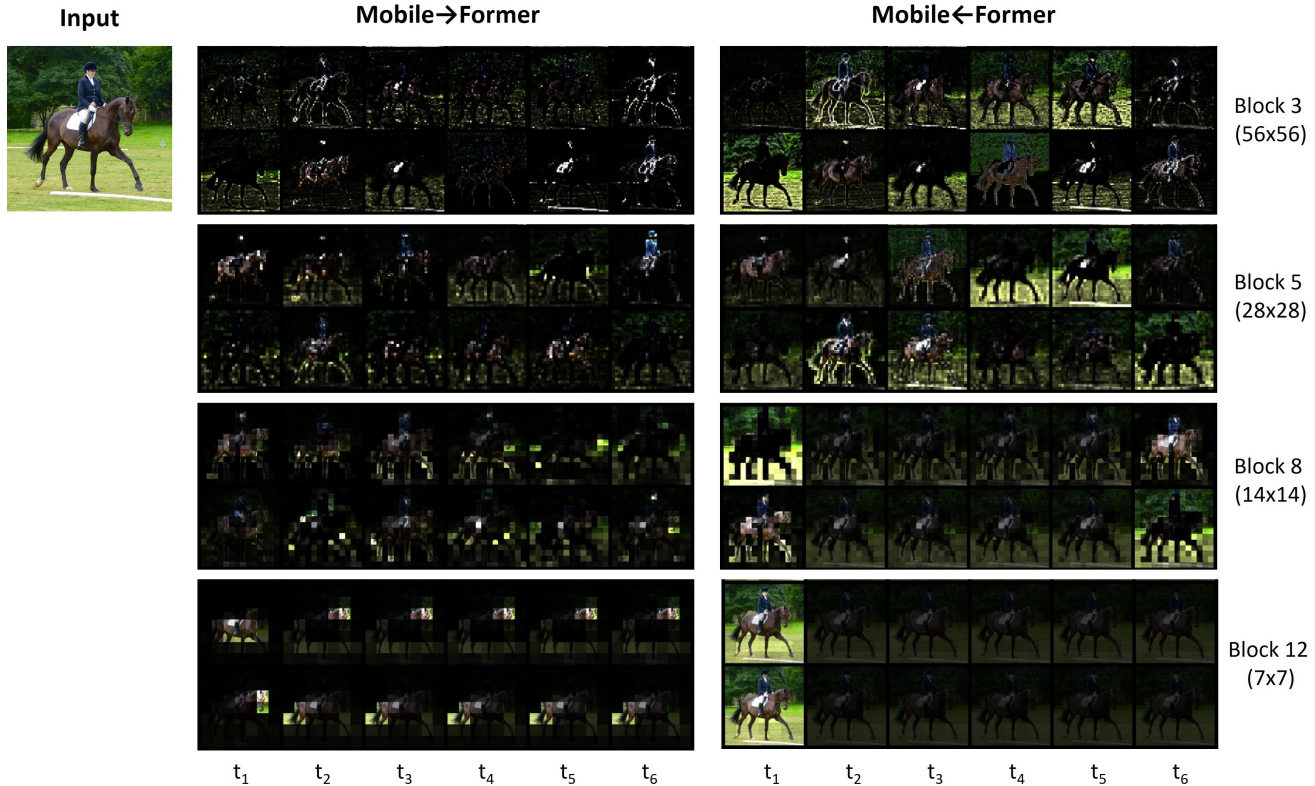


Figure 4. **Visualization of cross attention** on the two-way bridge: *Mobile→Former* and *Mobile←Former*. Mobile-Former-294M is used, which includes 6 tokens (each corresponds to a column). Four blocks with different input resolutions are selected and each has two attention heads that are visualized in two rows. Attention in *Mobile→Former* (left half) is normalized over pixels, showing the focused region per token. Attention in *Mobile←Former* (right half) is normalized over tokens showing the contribution per token at each pixel. The cross attention has more diversity across tokens at lower levels than higher levels. At the last block, token 2–5 have very similar cross attention.

bridge (*Mobile→Former* and *Mobile←Former*) in Figure 4, Figure 5 and Figure 6. The ImageNet pretrained Mobile-Former-294M is used, which includes 6 global tokens and 11 Mobile-Former blocks. We observe three interesting patterns.

First, the attention has more diversity across tokens at lower levels than higher levels. As shown in Figure 4, each column corresponds to a token, and each row corresponds to a head in the corresponding multi-head cross attention. Note that the attention is normalized over pixels in *Mobile→Former* (left half), showing the focused region per token. In contrast, the attention in *Mobile←Former* is normalized over tokens, comparing the contribution of different tokens at each pixel. Clearly, the six tokens at block 3 and 5 have different cross attention patterns in both *Mobile→Former* and *Mobile←Former*. Similar attention patterns among tokens is clearly observed at block 8. At block 12, the last five tokens share very similar attention pattern. Note that the first token is class token feed into the classifier head. The similar observation has been identified in recent studies on ViT [30, 45, 46].

Second, the focused regions of global tokens change progressively from low to high levels. Figure 5 shows the cross attention over pixels for the first token in *Mobile→Former*. This token begins focusing on local features, e.g. edges/corners (at block 2-4). Then it pays more attention to regions with connected pixels. Interestingly, the focused region shifts between foreground (person and horse) and background (grass) across blocks. Finally, it locates the most discriminative region (horse body and head) for classification.

Thirdly, the separation between foreground and background is surprisingly found at middle layers (e.g. block 8) of *Mobile←Former*. Figure 6 shows the cross attention over 6 tokens for each pixel at featuremap. Clearly, the foreground and background are separated by the first and last tokens. This shows that some global tokens learn meaningful prototypes that cluster similar pixels.

5.4. Limitations

The major limitation of Mobile-Former is the model size. This is due to two reasons. Firstly, the parallel design is not

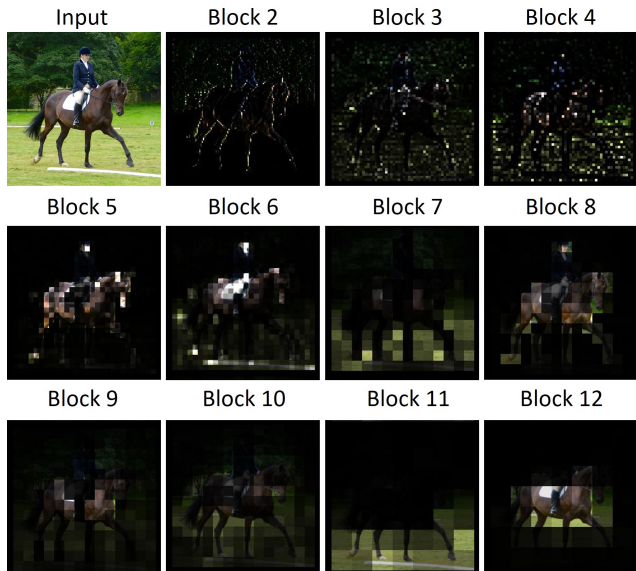


Figure 5. **Cross attention over featuremap for the first token in $Mobile \rightarrow Former$** across all Mobile-Former blocks. Attention is normalized over pixels, showing focused regions. The focused regions change from low to high levels. The token starts paying more attention to edges/corners at block 2–4. Then it focused more on bigger region rather than scattered small pieces at block 5–12. The focused region shifts between the foreground (person and horse) and background (grass). Finally, it locks the most discriminative part (horse body and head) for classification.

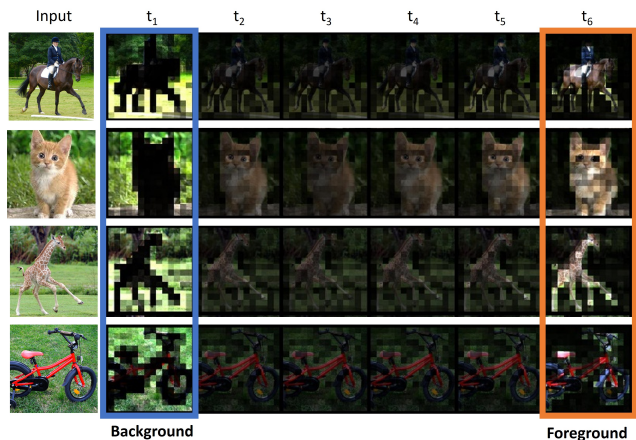


Figure 6. **Cross attention in $Mobile \leftarrow Former$ separates foreground and background at middle layers.** Attention is normalized over tokens showing the contribution of different tokens at each pixel. Block 8 is chosen where the background pixels pay more attention to the first token and the foreground pixels pay more attention to the last token.

efficient in terms of parameter sharing as *Mobile*, *Former* and bridge have their own parameters. Although *Former* is efficient in computation due to the small amount of to-

kens, but it does not save the number of parameters. Second, Mobile-Former consumes many parameters in the classification head (two fully connected layers) when performing ImageNet classification task. For instance, Mobile-Former-294M spends 40% (4.6M of 11.4M) parameters in the classification head. The model size problem mitigates when switching from image classification to object detection task, as the classification head is removed. We will explore the parameter efficiency in the future work.

6. Conclusion

This paper presents Mobile-Former, a new parallel design of MobileNet and Transformer with two-way bridge in between to communicate. It leverages the efficiency of MobileNet in local processing and the advantage of Transformer in encoding global interaction. This design is not only effective to boost accuracy, but also efficient to save computational cost. It outperforms both efficient CNNs and vision transformer variants on image classification and object detection in the low FLOP regime with a clear margin. We hope Mobile-Former encourage new design of efficient CNNs and transformers.

References

- [1] Hanqing Chen, Yunhe Wang, Chunjing Xu, Boxin Shi, Chao Xu, Qi Tian, and Chang Xu. Addnet: Do we really need multiplications in deep learning? In *Proceedings of the IEEE/CVF Conference on Computer Vision and Pattern Recognition (CVPR)*, June 2020. 2
- [2] Yinpeng Chen, Xiyang Dai, Mengchen Liu, Dongdong Chen, Lu Yuan, and Zicheng Liu. Dynamic convolution: Attention over convolution kernels. In *IEEE Conference on Computer Vision and Pattern Recognition (CVPR)*, 2020. 2
- [3] Yinpeng Chen, Xiyang Dai, Mengchen Liu, Dongdong Chen, Lu Yuan, and Zicheng Liu. Dynamic relu. In *ECCV*, 2020. 2, 3, 4, 6
- [4] Ekin D. Cubuk, Barret Zoph, Dandelion Mane, Vijay Vasudevan, and Quoc V. Le. Autoaugment: Learning augmentation strategies from data. In *Proceedings of the IEEE/CVF Conference on Computer Vision and Pattern Recognition (CVPR)*, June 2019. 5
- [5] Stéphane d’Ascoli, Hugo Touvron, Matthew Leavitt, Ari Morcos, Giulio Biroli, and Levent Sagun. Convit: Improving vision transformers with soft convolutional inductive biases. *arXiv preprint arXiv:2103.10697*, 2021. 2, 3, 5, 6
- [6] Jia Deng, Wei Dong, Richard Socher, Li-Jia Li, Kai Li, and Li Fei-Fei. Imagenet: A large-scale hierarchical image database. In *2009 IEEE conference on computer vision and pattern recognition*, pages 248–255. Ieee, 2009. 5, 6
- [7] Xiaoyi Dong, Jianmin Bao, Dongdong Chen, Weiming Zhang, Nenghai Yu, Lu Yuan, Dong Chen, and Baining Guo. Cswin transformer: A general vision transformer backbone with cross-shaped windows, 2021. 2
- [8] Alexey Dosovitskiy, Lucas Beyer, Alexander Kolesnikov, Dirk Weissenborn, Xiaohua Zhai, Thomas Unterthiner,

- Mostafa Dehghani, Matthias Minderer, Georg Heigold, Sylvain Gelly, Jakob Uszkoreit, and Neil Houlsby. An image is worth 16x16 words: Transformers for image recognition at scale. In *International Conference on Learning Representations*, 2021. 1, 2, 3
- [9] Benjamin Graham, Alaaeldin El-Nouby, Hugo Touvron, Pierre Stock, Armand Joulin, Hervé Jégou, and Matthijs Douze. Levit: a vision transformer in convnet’s clothing for faster inference. *arXiv preprint arXiv:22104.01136*, 2021. 1, 2, 3, 5
- [10] Kai Han, Yunhe Wang, Qi Tian, Jianyuan Guo, Chunjing Xu, and Chang Xu. Ghostnet: More features from cheap operations. In *IEEE/CVF Conference on Computer Vision and Pattern Recognition (CVPR)*, June 2020. 1, 2, 6
- [11] Kai Han, Yunhe Wang, Qiulin Zhang, Wei Zhang, Chunjing XU, and Tong Zhang. Model rubiks cube: Twisting resolution, depth and width for tinynets. In H. Larochelle, M. Ranzato, R. Hadsell, M. F. Balcan, and H. Lin, editors, *Advances in Neural Information Processing Systems*, volume 33, pages 19353–19364. Curran Associates, Inc., 2020. 2
- [12] Kaiming He, Xiangyu Zhang, Shaoqing Ren, and Jian Sun. Deep residual learning for image recognition. In *Proceedings of the IEEE conference on computer vision and pattern recognition*, pages 770–778, 2016. 3, 6, 7
- [13] Geoffrey E. Hinton. How to represent part-whole hierarchies in a neural network. *CoRR*, abs/2102.12627, 2021. 2
- [14] Andrew Howard, Mark Sandler, Grace Chu, Liang-Chieh Chen, Bo Chen, Mingxing Tan, Weijun Wang, Yukun Zhu, Ruoming Pang, Vijay Vasudevan, Quoc V. Le, and Hartwig Adam. Searching for mobilenetv3. In *Proceedings of the IEEE/CVF International Conference on Computer Vision (ICCV)*, October 2019. 1, 2, 4, 5, 6, 7
- [15] Andrew G Howard, Menglong Zhu, Bo Chen, Dmitry Kalenichenko, Weijun Wang, Tobias Weyand, Marco Andreetto, and Hartwig Adam. Mobilenets: Efficient convolutional neural networks for mobile vision applications. *arXiv preprint arXiv:1704.04861*, 2017. 1, 2
- [16] Jie Hu, Li Shen, and Gang Sun. Squeeze-and-excitation networks. In *The IEEE Conference on Computer Vision and Pattern Recognition (CVPR)*, June 2018. 2
- [17] Yunsheng Li, Yinpeng Chen, Xiyang Dai, Dongdong Chen, Mengchen Liu, Lu Yuan, Zicheng Liu, Lei Zhang, and Nuno Vasconcelos. Micronet: Improving image recognition with extremely low flops. In *International Conference on Computer Vision*, 2021. 1, 2, 4, 12
- [18] Tsung-Yi Lin, Priya Goyal, Ross Girshick, Kaiming He, and Piotr Dollar. Focal loss for dense object detection. In *Proceedings of the IEEE International Conference on Computer Vision (ICCV)*, Oct 2017. 6
- [19] Tsung-Yi Lin, Michael Maire, Serge Belongie, James Hays, Pietro Perona, Deva Ramanan, Piotr Dollár, and C Lawrence Zitnick. Microsoft coco: Common objects in context. In *European conference on computer vision*, pages 740–755. Springer, 2014. 5, 6
- [20] Ze Liu, Yutong Lin, Yue Cao, Han Hu, Yixuan Wei, Zheng Zhang, Stephen Lin, and Baining Guo. Swin transformer: Hierarchical vision transformer using shifted windows. *arXiv preprint arXiv:2103.14030*, 2021. 2, 5, 6
- [21] Ilya Loshchilov and Frank Hutter. Decoupled weight decay regularization. In *International Conference on Learning Representations*, 2019. 5
- [22] Ningning Ma, X. Zhang, J. Huang, and J. Sun. Weightnet: Revisiting the design space of weight networks. volume abs/2007.11823, 2020. 5
- [23] Ningning Ma, Xiangyu Zhang, Hai-Tao Zheng, and Jian Sun. Shufflenet v2: Practical guidelines for efficient cnn architecture design. In *The European Conference on Computer Vision (ECCV)*, September 2018. 2, 5, 6, 7
- [24] Mark Sandler, Andrew Howard, Menglong Zhu, Andrey Zhmoginov, and Liang-Chieh Chen. Mobilenetv2: Inverted residuals and linear bottlenecks. In *Proceedings of the IEEE Conference on Computer Vision and Pattern Recognition*, pages 4510–4520, 2018. 1, 2, 3, 4
- [25] Aravind Srinivas, Tsung-Yi Lin, Niki Parmar, Jonathon Shlens, Pieter Abbeel, and Ashish Vaswani. Bottleneck transformers for visual recognition. In *Proceedings of the IEEE/CVF Conference on Computer Vision and Pattern Recognition (CVPR)*, pages 16519–16529, June 2021. 2, 3, 6
- [26] Mingxing Tan and Quoc Le. Efficientnet: Rethinking model scaling for convolutional neural networks. In *ICML*, pages 6105–6114, Long Beach, California, USA, 09–15 Jun 2019. 2, 5
- [27] Mingxing Tan and Quoc V. Le. Mixconv: Mixed depthwise convolutional kernels. In *30th British Machine Vision Conference 2019*, 2019. 2
- [28] Mingxing Tan, Ruoming Pang, and Quoc V. Le. Efficientdet: Scalable and efficient object detection. In *Proceedings of the IEEE/CVF Conference on Computer Vision and Pattern Recognition (CVPR)*, June 2020. 2
- [29] Hugo Touvron, Matthieu Cord, Matthijs Douze, Francisco Massa, Alexandre Sablayrolles, and Hervé Jégou. Training data-efficient image transformers and distillation through attention. *arXiv preprint arXiv:2012.12877*, 2020. 1, 2, 5, 6
- [30] Hugo Touvron, Matthieu Cord, Alexandre Sablayrolles, Gabriel Synnaeve, and Hervé Jégou. Going deeper with image transformers, 2021. 8
- [31] Keivan Alizadeh vahid, Anish Prabhu, Ali Farhadi, and Mohammad Rastegari. Butterfly transform: An efficient fft based neural architecture design. In *Proceedings of the IEEE/CVF Conference on Computer Vision and Pattern Recognition (CVPR)*, June 2020. 2
- [32] Ashish Vaswani, Prajit Ramachandran, Aravind Srinivas, Niki Parmar, Blake Hechtman, and Jonathon Shlens. Scaling local self-attention for parameter efficient visual backbones. In *Proceedings of the IEEE/CVF Conference on Computer Vision and Pattern Recognition (CVPR)*, pages 12894–12904, June 2021. 2
- [33] Ashish Vaswani, Noam Shazeer, Niki Parmar, Jakob Uszkoreit, Llion Jones, Aidan N Gomez, Łukasz Kaiser, and Illia Polosukhin. Attention is all you need. In I. Guyon, U. V. Luxburg, S. Bengio, H. Wallach, R. Fergus, S. Vishwanathan, and R. Garnett, editors, *Advances in Neural Information Processing Systems*, volume 30. Curran Associates, Inc., 2017. 1, 3, 4

- [34] Wenhai Wang, Enze Xie, Xiang Li, Deng-Ping Fan, Kaitao Song, Ding Liang, Tong Lu, Ping Luo, and Ling Shao. Pyramid vision transformer: A versatile backbone for dense prediction without convolutions, 2021. [5](#), [6](#), [7](#)
- [35] Haiping Wu, Bin Xiao, Noel Codella, Mengchen Liu, Xiyang Dai, Lu Yuan, and Lei Zhang. Cvt: Introducing convolutions to vision transformers, 2021. [1](#), [2](#), [3](#)
- [36] Tete Xiao, Mannat Singh, Eric Mintun, Trevor Darrell, Piotr Dollár, and Ross B. Girshick. Early convolutions help transformers see better. *CoRR*, abs/2106.14881, 2021. [1](#), [2](#), [3](#), [5](#), [6](#)
- [37] Weijian Xu, Yifan Xu, Tyler Chang, and Zhuowen Tu. Co-scale conv-attentional image transformers, 2021. [5](#), [6](#)
- [38] Haotian Yan, Zhe Li, Weijian Li, Changhu Wang, Ming Wu, and Chuang Zhang. Contnet: Why not use convolution and transformer at the same time? *CoRR*, abs/2104.13497, 2021. [6](#), [7](#)
- [39] Brandon Yang, Gabriel Bender, Quoc V. Le, and Jiquan Ngiam. Condconv: Conditionally parameterized convolutions for efficient inference. In *NeurIPS*, 2019. [2](#)
- [40] Li Yuan, Yunpeng Chen, Tao Wang, Weihao Yu, Yujun Shi, Francis EH Tay, Jiashi Feng, and Shuicheng Yan. Tokens-to-token vit: Training vision transformers from scratch on imagenet. *arXiv preprint arXiv:2101.11986*, 2021. [2](#), [5](#), [6](#)
- [41] Hongyi Zhang, Moustapha Cisse, Yann N. Dauphin, and David Lopez-Paz. mixup: Beyond empirical risk minimization. In *International Conference on Learning Representations*, 2018. [5](#)
- [42] Xiangyu Zhang, Xinyu Zhou, Mengxiao Lin, and Jian Sun. Shufflenet: An extremely efficient convolutional neural network for mobile devices. In *The IEEE Conference on Computer Vision and Pattern Recognition (CVPR)*, June 2018. [2](#)
- [43] Zhun Zhong, Liang Zheng, Guoliang Kang, Shaozi Li, and Yi Yang. Random erasing data augmentation. In *Proceedings of the AAAI Conference on Artificial Intelligence (AAAI)*, 2020. [5](#)
- [44] Daquan Zhou, Qi-Bin Hou, Y. Chen, Jiashi Feng, and S. Yan. Rethinking bottleneck structure for efficient mobile network design. In *ECCV*, August 2020. [2](#)
- [45] Daquan Zhou, Bingyi Kang, Xiaojie Jin, Linjie Yang, Xiaochen Lian, Zihang Jiang, Qibin Hou, and Jiashi Feng. Deepvit: Towards deeper vision transformer, 2021. [8](#)
- [46] Daquan Zhou, Yujun Shi, Bingyi Kang, Weihao Yu, Zihang Jiang, Yuan Li, Xiaojie Jin, Qibin Hou, and Jiashi Feng. Refiner: Refining self-attention for vision transformers, 2021. [8](#)

Stage	Mobile-Former-508M			Mobile-Former-294M			Mobile-Former-214M			Mobile-Former-151M			Mobile-Former-96M			Mobile-Former-52M		
	Block	#exp	#out	Block	#exp	#out	Block	#exp	#out									
token	6×192			6×192			6×192			6×192			4×128			3×128		
stem	conv 3×3	–	24	conv 3×3	–	16	conv 3×3	–	12	conv 3×3	–	12	conv 3×3	–	12	conv 3×3	–	8
1	bneck-lite	48	24	bneck-lite	32	16	bneck-lite	24	12	bneck-lite	24	12	bneck-lite	24	12			
2	M-F [↓]	144	40	M-F [↓]	96	24	M-F [↓]	72	20	M-F [↓]	72	16	M-F [↓]	72	16	bneck-lite [↓]	24	12
	M-F	120	40	M-F	96	24	M-F	60	20	M-F	48	16	M-F	48	16	M-F	36	12
3	M-F [↓]	240	72	M-F [↓]	144	48	M-F [↓]	120	40	M-F [↓]	96	32	M-F [↓]	96	32	M-F [↓]	72	24
	M-F	216	72	M-F	192	48	M-F	160	40	M-F	96	32	M-F	96	32	M-F	72	24
4	M-F [↓]	432	128	M-F [↓]	288	96	M-F [↓]	240	80	M-F [↓]	192	64	M-F [↓]	192	64	M-F [↓]	144	48
	M-F	512	128	M-F	384	96	M-F	320	80	M-F	256	64	M-F	256	64	M-F	192	48
	M-F	768	176	M-F	576	128	M-F	480	112	M-F	384	88	M-F	384	88	M-F	288	64
	M-F	1056	176	M-F	768	128	M-F	672	112	M-F	528	88	M-F	528	88			
5	M-F [↓]	1056	240	M-F [↓]	768	192	M-F [↓]	672	160	M-F [↓]	528	128	M-F [↓]	528	128	M-F [↓]	384	96
	M-F	1440	240	M-F	1152	192	M-F	960	160	M-F	768	128	M-F	768	128	M-F	576	96
	M-F	1440	240	M-F	1152	192	M-F	960	160	M-F	768	128	M-F	768	128	conv 1×1	–	768
	conv 1×1	–	1440	conv 1×1	–	1152	conv 1×1	–	960	conv 1×1	–	768				conv 1×1	–	576
pool	–	–	1632	–	–	1344	–	–	1152	–	–	960	–	–	896	–	–	704
concat	–	–	1920	–	–	1920	–	–	1600	–	–	1280	–	–	1280	–	–	1024
FC1	–	–	1000	–	–	1000	–	–	1000	–	–	1000	–	–	1000	–	–	1000
FC2	–	–	1000	–	–	1000	–	–	1000	–	–	1000	–	–	1000	–	–	1000

Table 10. **Specification of Mobile-Former Models.** “bneck-lite” denotes light bottleneck block [17]. “M-F” denotes the Mobile-Former block and “M-F[↓]” denotes the Mobile-Former block with downsampling. Mobile-Former-26M has similar architecture to Mobile-Former-52M except replacing all 1×1 convolution with group convolution (group=4).

A. Mobile-Former Architectures

Table 10 shows six Mobile-Former models (508M–52M). These models are manually designed without searching for the optimal architecture parameters (e.g. width or depth). We follow the well known rules used in MobileNet: (a) the number of channels increases across stages, and (b) channel expansion rate starts with three at low levels and increases to six at high levels. For the four bigger models (508M–151M), we use six global tokens with dimension 192 and 11 Mobile-Former blocks. But these four models have different widths. Mobile-Former-96M and Mobile-Former-52M are shallower (with only 8 Mobile-Former blocks) to meet the low computational budget. Mobile-Former-26M has similar architecture to Mobile-Former-52M except replacing all 1×1 convolution with group convolution (group=4).

B. Training Hyper-Parameters

Table 11 shows three hyper-parameters (learning rate, weight decay and dropout rate) on ImageNet classification for all Mobile-Former models. Their values increase as the model becomes bigger to prevent overfitting.

C. Visualization

We visualize the cross attention on the two-way bridge (*Mobile*→*Former* and *Mobile*←*Former*) for all blocks in Figure 7. We use ImageNet pretrained Mobile-Former-294M, which includes 6 global tokens and 11 Mobile-Former blocks. In Figure 7, each column corresponds to

Model	Learning Rate	Weight Decay	Dropout
Mobile-Former-26M	8e-4	0.08	0.1
Mobile-Former-52M	8e-4	0.10	0.2
Mobile-Former-96M	8e-4	0.10	0.2
Mobile-Former-151M	9e-4	0.10	0.2
Mobile-Former-214M	9e-4	0.15	0.2
Mobile-Former-294M	1e-3	0.20	0.3
Mobile-Former-508M	1e-3	0.20	0.3

Table 11. **Hyper-parameters** of Mobile-Former models for ImageNet classification.

a token, and each row corresponds to a head in the corresponding multi-head cross attention. Note that the attention is normalized over pixels in *Mobile*→*Former* (left half), showing the focused region per token. In contrast, the attention in *Mobile*←*Former* is normalized over tokens. For instance, at the second head of block 5 in *Mobile*←*Former*, pixels on the person and horse attend more on the second token while pixels on the background attend more on the last token.

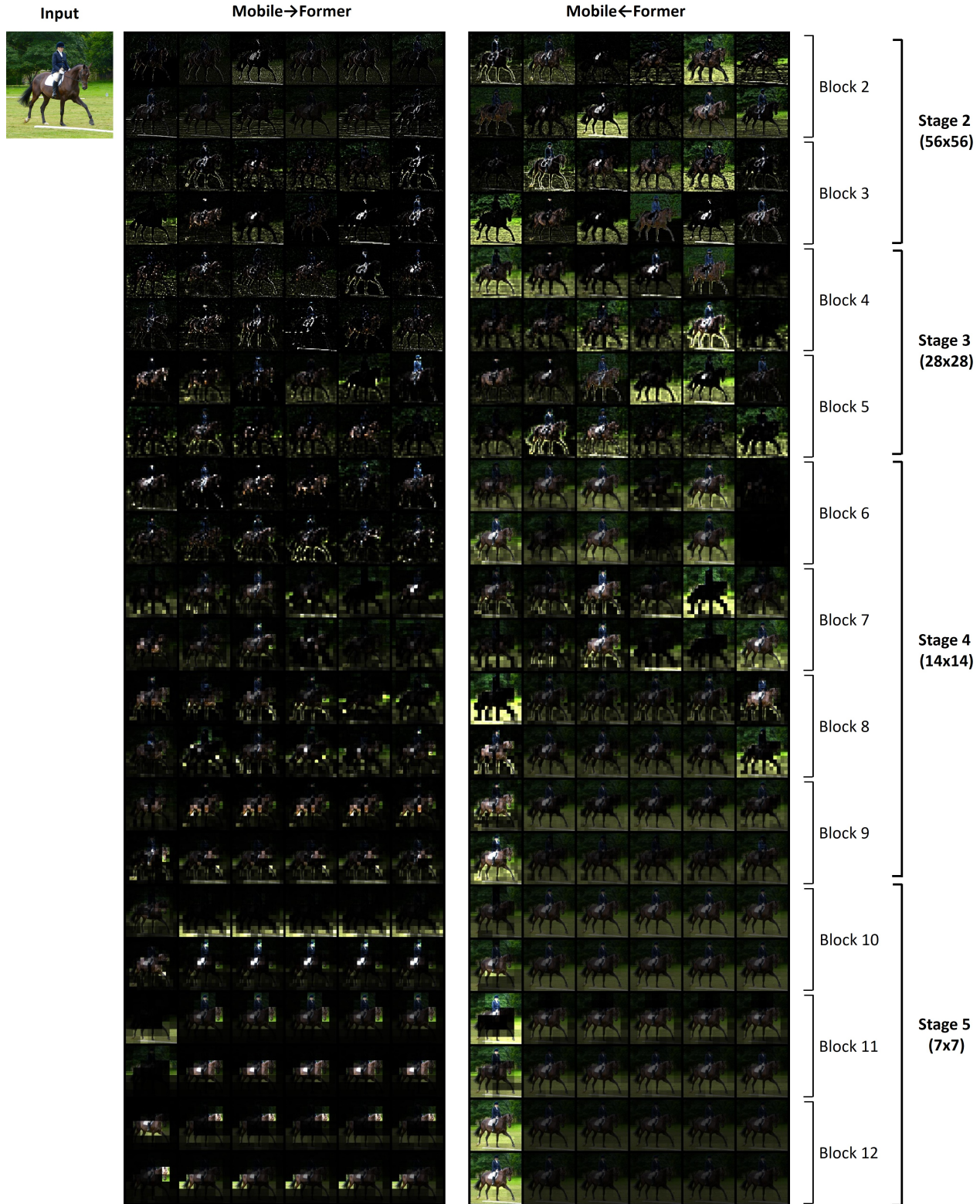


Figure 7. **Visualization of cross attention** on the two-way bridge: *Mobile→Former* and *Mobile←Former*. Mobile-Former-294M is used, which includes 6 tokens (each corresponds to a column) and 11 Mobile-Former blocks (block 2–12) across 4 stages. Each block has two attention heads that are visualized in two rows. Attention in *Mobile→Former* (left half) is normalized over pixels, showing the focused region per token. Attention in *Mobile←Former* (right half) is normalized over tokens showing the contribution per token at each pixel.